Gravitational Wave Physics and Astronomy Genesis

IBS Workshop on
Prospects of Particle Physics and Cosmology

Testing gravity theory using gravitational waves

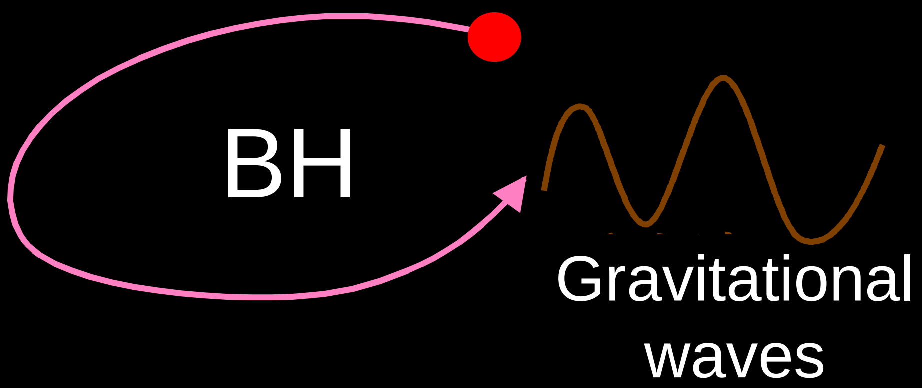

Takahiro Tanaka
(Dept. of Phys./YITP
Kyoto university)

Our new Innovative Area (grant) has just started from the last summer.

Synergy between data analysis and theory researches

A: BH binaries
A-01
Testing gravity using gravitational waves
A-02
Gravity and Cosmology
A-03
BH binary formation

B: NS binaries
B-01
Internal structure of NS
B-02
Gamma-ray burst and BH
B-03
r –process elements

C: Supernovae
C-01
SN explosion mechanism
C-02
SN explosion mechanism via ν observation

Physics and astronomy motivated by GW observations

Motivation for considering modified gravity

1) Incompleteness of General relativity

GR is non-renormalizable

Singularity formation after gravitational collapse

2) Dark energy problem

3) To test General relativity

GR has been repeatedly tested since its first proposal.

The precision of the test is getting higher and higher.

$\Rightarrow$ Do we need to understand what kind of modification is theoretically possible before experimental test?

Yes, especially in the era of gravitational wave observation!

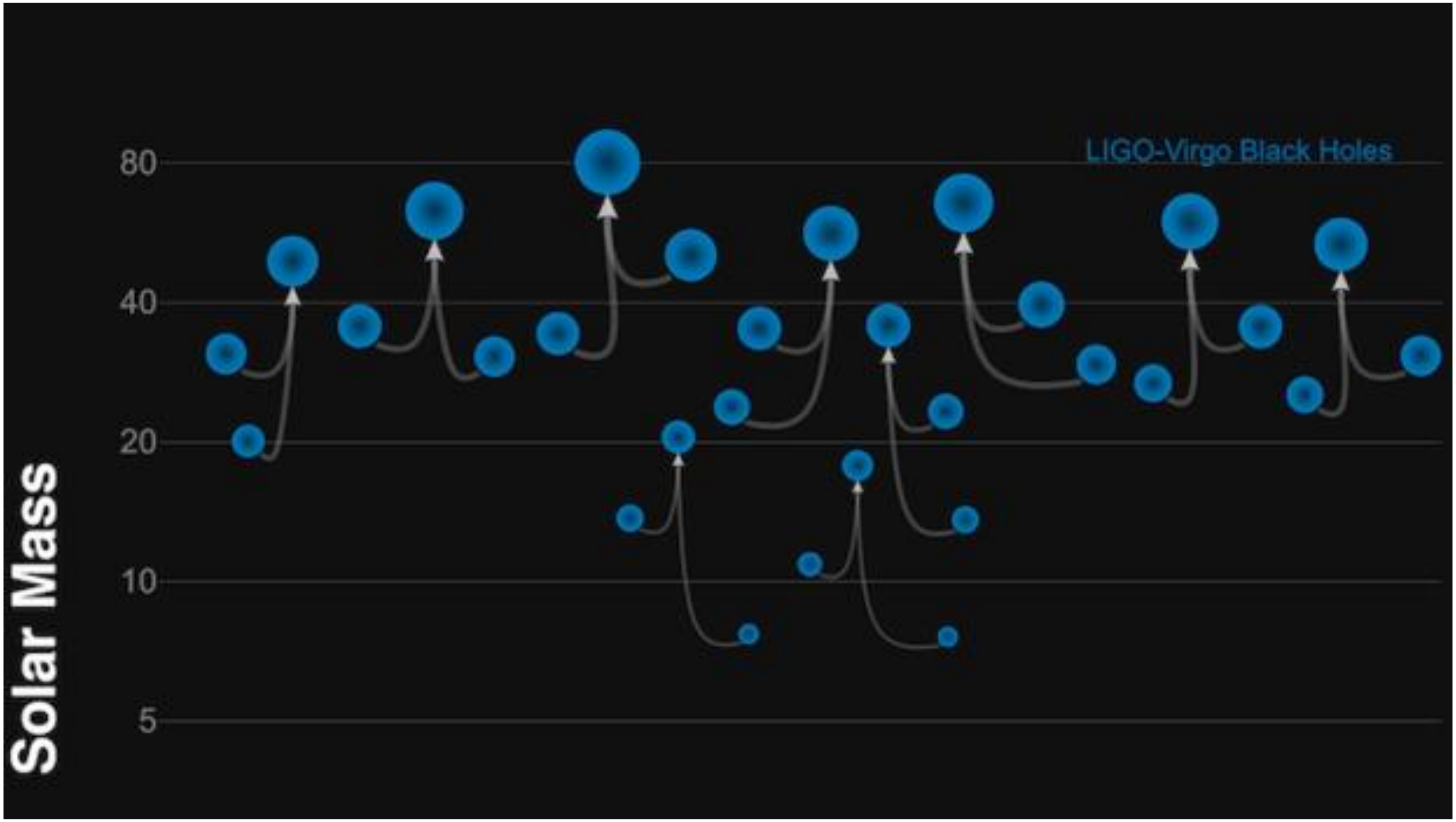
LIGO-Virgo Black Holes
Solar Mass
80
40
20
10
5

Event	$m_1/\mathrm{M}_\odot$	$m_2/\mathrm{M}_\odot$	$\mathcal{M}/\mathrm{M}_\odot$	χ_{eff}	$M_{\mathrm{f}}/\mathrm{M}_\odot$	a_{f}	$E_{\mathrm{rad}}/(\mathrm{M}_\odot c^2)$	$\ell_{\mathrm{peak}}/(\mathrm{erg\,s^{-1}})$	d_L/Mpc	z	$\Delta\Omega/\mathrm{deg}^2$	Network SNR GstLAL
GW150914	$35.6^{+4.8}_{-3.0}$	$30.6^{+3.0}_{-4.4}$	$28.6^{+1.6}_{-1.5}$	$-0.01^{+0.12}_{-0.13}$	$63.1^{+3.3}_{-3.0}$	$0.69^{+0.05}_{-0.04}$	$3.1^{+0.4}_{-0.4}$	$3.6^{+0.4}_{-0.4}\times 10^{56}$	430^{+150}_{-170}	$0.09^{+0.03}_{-0.03}$	179	24.4
GW151012	$23.3^{+14.0}_{-5.5}$	$13.6^{+4.1}_{-4.8}$	$15.2^{+2.0}_{-1.1}$	$0.04^{+0.28}_{-0.19}$	$35.7^{+9.9}_{-3.8}$	$0.67^{+0.13}_{-0.11}$	$1.5^{+0.5}_{-0.5}$	$3.2^{+0.8}_{-1.7}\times 10^{56}$	1060^{+540}_{-480}	$0.21^{+0.09}_{-0.09}$	1555	10.0
GW151226	$13.7^{+8.8}_{-3.2}$	$7.7^{+2.2}_{-2.6}$	$8.9^{+0.3}_{-0.3}$	$0.18^{+0.20}_{-0.12}$	$20.5^{+6.4}_{-1.5}$	$0.74^{+0.07}_{-0.05}$	$1.0^{+0.1}_{-0.2}$	$3.4^{+0.7}_{-1.7}\times 10^{56}$	440^{+180}_{-190}	$0.09^{+0.04}_{-0.04}$	1033	13.1
GW170104	$31.0^{+7.2}_{-5.6}$	$20.1^{+4.9}_{-4.5}$	$21.5^{+2.1}_{-1.7}$	$-0.04^{+0.17}_{-0.20}$	$49.1^{+5.2}_{-3.9}$	$0.66^{+0.08}_{-0.10}$	$2.2^{+0.5}_{-0.5}$	$3.3^{+0.6}_{-0.9}\times 10^{56}$	960^{+430}_{-410}	$0.19^{+0.07}_{-0.08}$	924	13.0
GW170608	$10.9^{+5.3}_{-1.7}$	$7.6^{+1.3}_{-2.1}$	$7.9^{+0.2}_{-0.2}$	$0.03^{+0.19}_{-0.07}$	$17.8^{+3.2}_{-0.7}$	$0.69^{+0.04}_{-0.04}$	$0.9^{+0.0}_{-0.1}$	$3.5^{+0.4}_{-1.3}\times 10^{56}$	320^{+120}_{-110}	$0.07^{+0.02}_{-0.02}$	396	14.9
GW170729	$50.6^{+16.6}_{-10.2}$	$34.3^{+9.1}_{-10.1}$	$35.7^{+6.5}_{-4.7}$	$0.36^{+0.21}_{-0.25}$	$80.3^{+14.6}_{-10.2}$	$0.81^{+0.07}_{-0.13}$	$4.8^{+1.7}_{-1.7}$	$4.2^{+0.9}_{-1.5}\times 10^{56}$	2750^{+1350}_{-1320}	$0.48^{+0.19}_{-0.20}$	1033	10.8
GW170809	$35.2^{+8.3}_{-6.0}$	$23.8^{+5.2}_{-5.1}$	$25.0^{+2.1}_{-1.6}$	$0.07^{+0.16}_{-0.16}$	$56.4^{+5.2}_{-3.7}$	$0.70^{+0.08}_{-0.09}$	$2.7^{+0.6}_{-0.6}$	$3.5^{+0.6}_{-0.9}\times 10^{56}$	990^{+320}_{-380}	$0.20^{+0.05}_{-0.07}$	340	12.4
GW170814	$30.7^{+5.7}_{-3.0}$	$25.3^{+2.9}_{-4.1}$	$24.2^{+1.4}_{-1.1}$	$0.07^{+0.12}_{-0.11}$	$53.4^{+3.2}_{-2.4}$	$0.72^{+0.07}_{-0.05}$	$2.7^{+0.4}_{-0.3}$	$3.7^{+0.4}_{-0.5}\times 10^{56}$	580^{+160}_{-210}	$0.12^{+0.03}_{-0.04}$	87	15.9
GW170817	$1.46^{+0.12}_{-0.10}$	$1.27^{+0.09}_{-0.09}$	$1.186^{+0.001}_{-0.001}$	$0.00^{+0.02}_{-0.01}$	≤ 2.8	≤ 0.89	≥ 0.04	$\geq 0.1\times 10^{56}$	40^{+10}_{-10}	$0.01^{+0.00}_{-0.00}$	16	33.0
GW170818	$35.5^{+7.5}_{-4.7}$	$26.8^{+4.3}_{-5.2}$	$26.7^{+2.1}_{-1.7}$	$-0.09^{+0.18}_{-0.21}$	$59.8^{+4.8}_{-3.8}$	$0.67^{+0.07}_{-0.08}$	$2.7^{+0.5}_{-0.5}$	$3.4^{+0.5}_{-0.7}\times 10^{56}$	1020^{+430}_{-360}	$0.20^{+0.07}_{-0.07}$	39	11.3
GW170823	$39.6^{+10.0}_{-6.6}$	$29.4^{+6.3}_{-7.1}$	$29.3^{+4.2}_{-3.2}$	$0.08^{+0.20}_{-0.22}$	$65.6^{+9.4}_{-6.6}$	$0.71^{+0.08}_{-0.10}$	$3.3^{+0.9}_{-0.8}$	$3.6^{+0.6}_{-0.9}\times 10^{56}$	1850^{+840}_{-840}	$0.34^{+0.13}_{-0.14}$	1651	11.5

arXiv:1811.12907

GW150914 and also GW170817(BNS) have extra-ordinarily high S/N.

Only GW151226 and GW170729 weakly suggest the existence of spin before merger.

What we can say from these GW events?

- Direct detection of GWs
  - Really detected
    - GWs really propagate.
- Existence of $30M_{sol}$ black holes
  - Moreover, they are rather abundant.
    - 0.6-12events/year/Gpc^3
- Are these “BHs” still BH candidates or BHs?

Judging whether they are BHs or BH candidates is difficult, but

- No big discrepancy between theoretical predictions and observations will indicate certainly more than the previous argument based on observations of matter accretion onto BHs.

“Many people will think these objects are BHs but it would be more conclusive if QNM modes are detected as expected. ”

BH quasi-normal mode (QNM)

≈

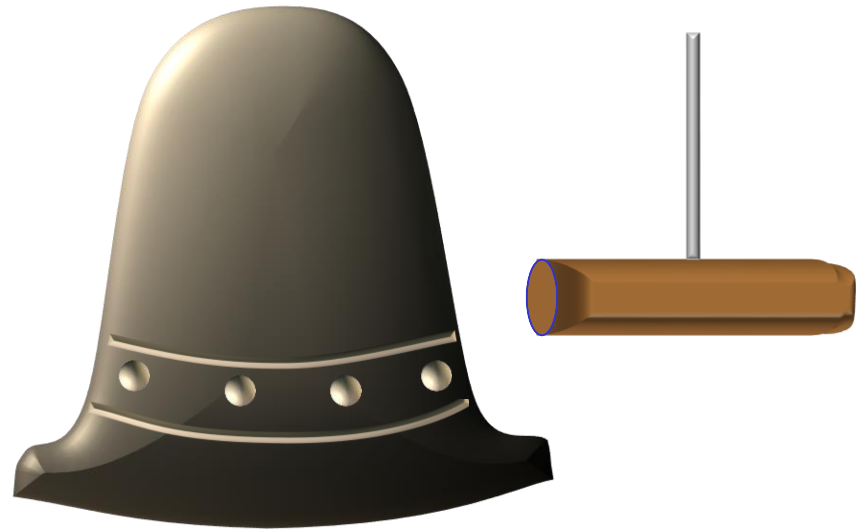

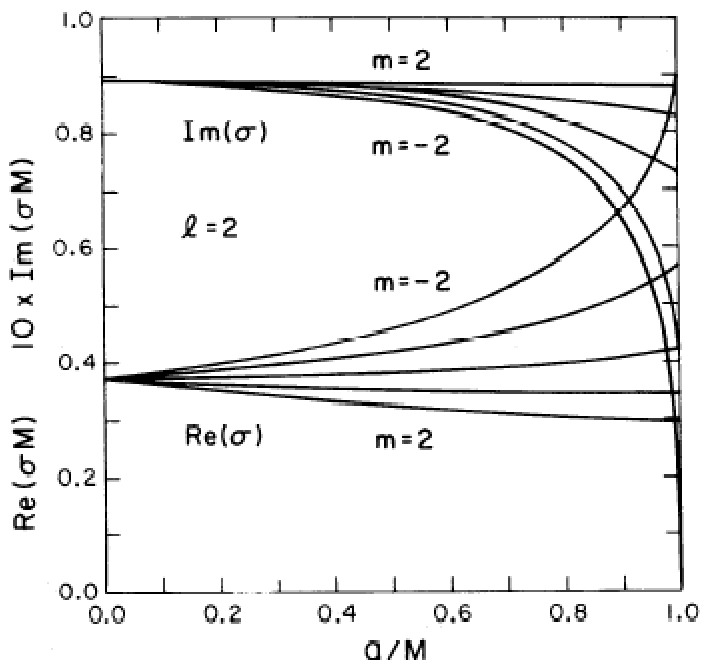

Frequency (f_R) and damping rate (f_I) are determined by the BH mass and spin.

Evidence for the formation of BH

(Detweiler ApJ239 292 (1980))

How deeply can we see BH spacetime by observing QNMs?

$$\approx \exp(-ik(t+r_*))$$

near horizon

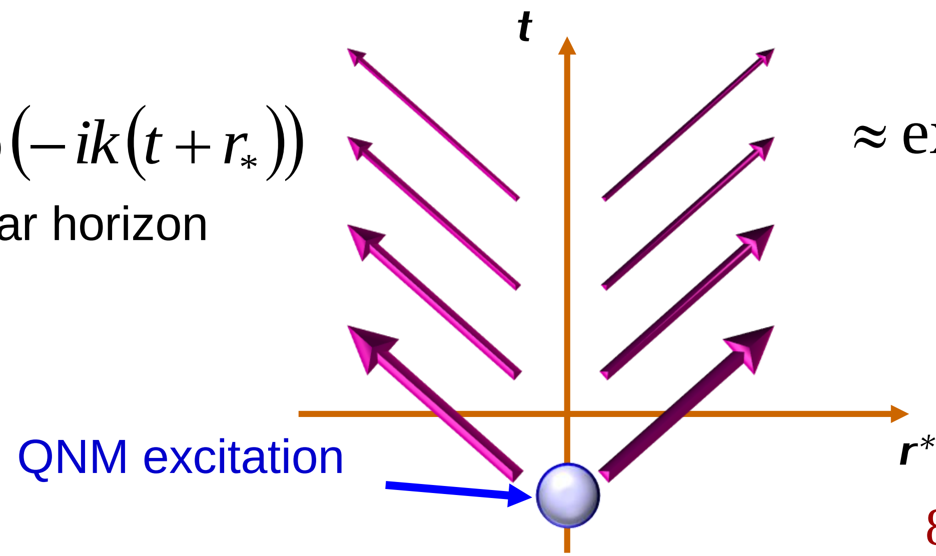

$$\approx \exp(-i\omega(t-r_*))$$

near infinity

• QNM frequencies can be rather accurately obtained by WKB approximation (Schutz &Will, ApJ, 291 (1985))

• But breakdown of WKB approx. is necessary to find a solution connecting in-going and out-going waves.

• The breakdown of WKB approx. occurs at around the extremum of the effective potential V.

• In WKB approx. the behavior of V around the extremum determines the QNMs

• The position of the extremum of V will give an approximate answer to the above question.

(Nakamura et al., Phys.Rev. D93 (2016))

$$(\omega_r + i\omega_i)^2 = V_{\mathrm{D}}(r_0^*) - i\sqrt{-\frac{1}{2}\frac{d^2V_{\mathrm{D}}}{dr^{*2}}\Big|_{r^*=r_0^*}}$$

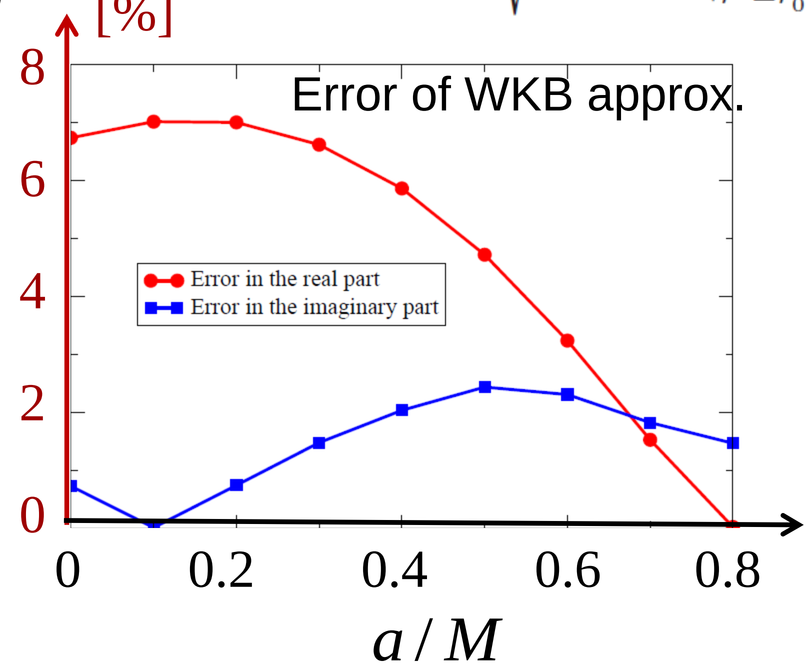

(Nakamura, Nakano, TT arXiv:1601.00356)

How deeply can we see BH spacetime by observing QNMs?

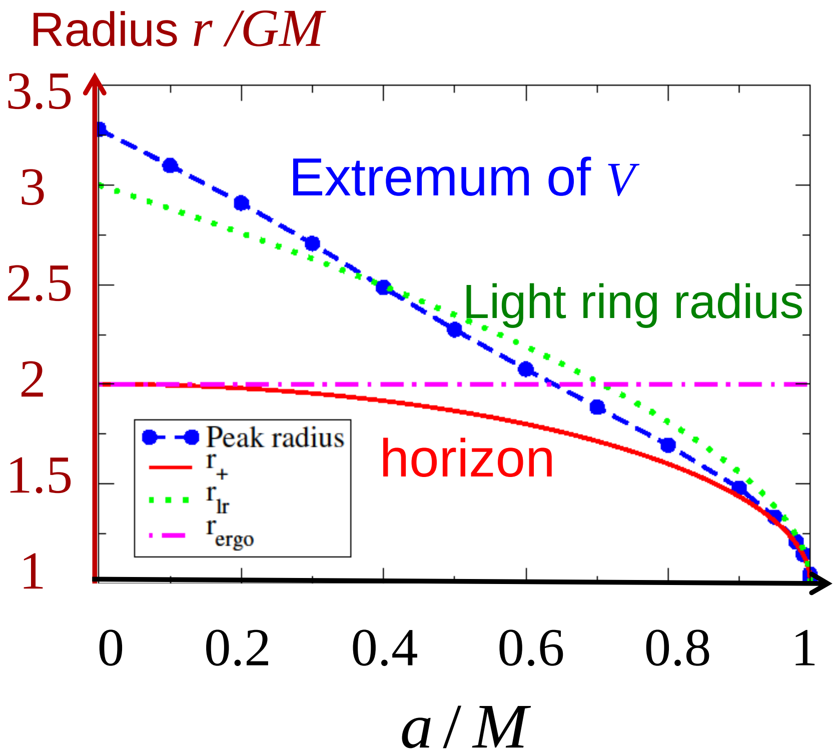

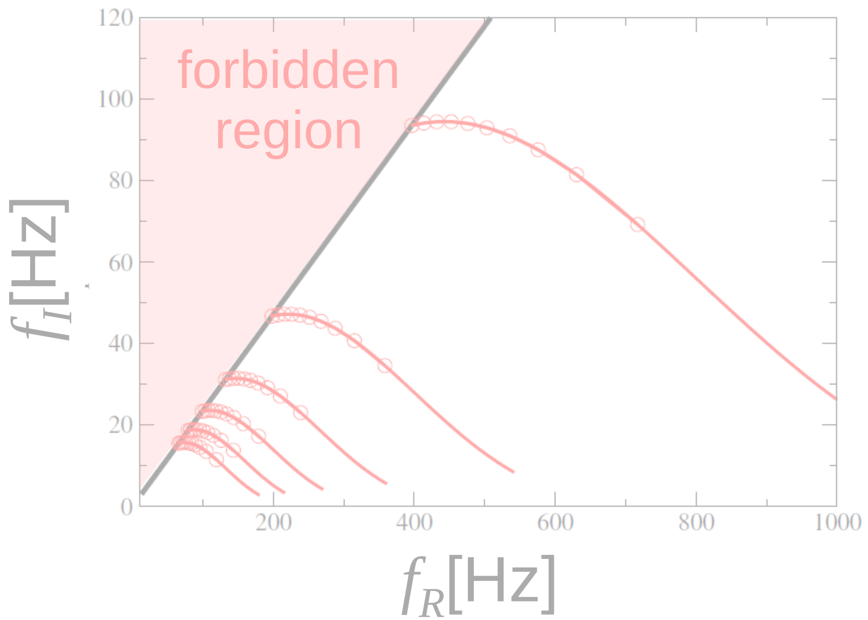

- Potential maximum that determines QNM frequency is rather close to horizon, especially for rapidly rotating case.

(Nakamura, Nakano, arXiv:1602.02385)

- There is a forbidden region for QNM frequencies in GR
- Black line is corresponding to Schwarzschild case

(Nakano, TT, Nakamura, arXiv:1506.00560)

Mock data challenge

H. Nakano, T. Narikawa, K. Ohara, K. Sakai, H. Shinkai,
H. Tagoshi, H. Takahashi, N. Uchikata, S. Yamamoto, T. Yamamoto
arXiv:1811.06443

- Many groups have been working on extracting QNMs as a test of performance of advanced data analysis methods.
- But fair comparison of performance has not been done.

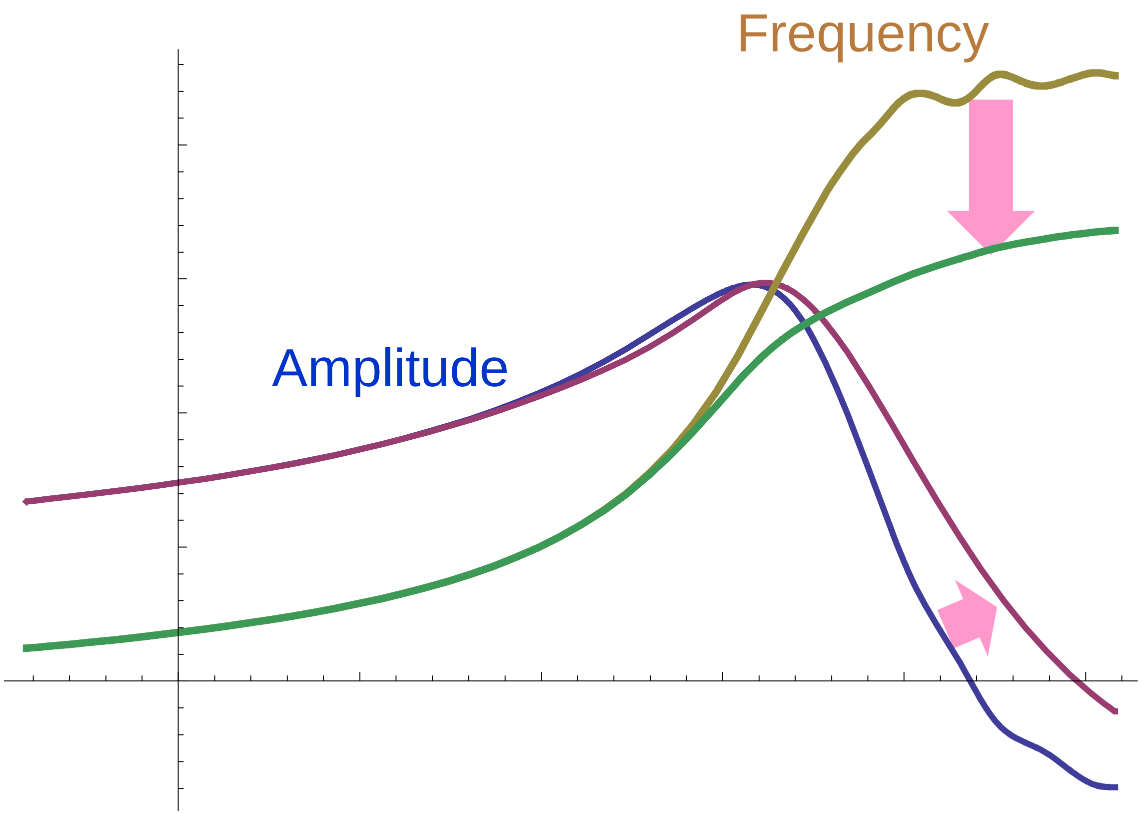

Numerical relativity simulation tells that the evolution of frequency and amplitude in GR is rather simple and smooth.

⇒ We construct waveform with modified f_R and f_I with Gaussian noise.

Then, can we extract f_R and f_I?

Mock data challenge

- Many groups have been working on extracting QNMs as a test of performance of advanced data analysis methods.
- But fair comparison of performance has not been done.

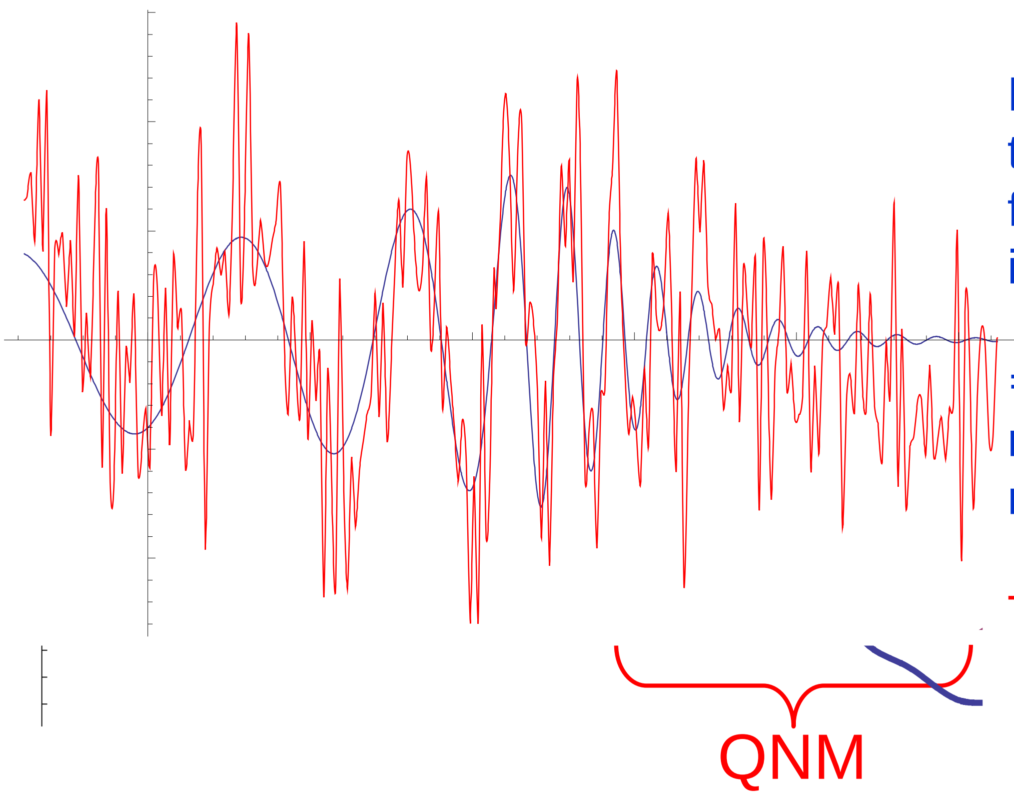

Numerical relativity simulation tells that the evolution of frequency and amplitude in GR is rather simple and smooth.

⇒We construct waveform with modified f_R and f_I with Gaussian noise.

Then, can we extract f_R and f_I?

Matched filtering

$$\left(s\,|\,h\right) \approx \int \frac{df}{S_n\left(f\right)} s\left(f\right) h^*\left(f\right)$$

s: data
h: template with parameter $\boldsymbol{\theta}$
$S_n(f) := 2\int_{-\infty}^{+\infty} d\tau \langle n(t) n(t+\tau) \rangle e^{2\pi i f \tau}$
n: noise

Find parameter $\boldsymbol{\theta}$ that realizes maximum $(s|h)$.

- Matched filtering is the optimal one among linear filtering methods for Gaussian noise.
- However, it is not generally guaranteed to be optimal.
- Also, the estimate of QNM frequency based on matched filtering might be systematically biased depending on the assumed wave form.

Ohara, Sakai, Takahashi

Empirical Mode decomposition

We drop high and low frequency modes by filtering the data [f_L, f_H]

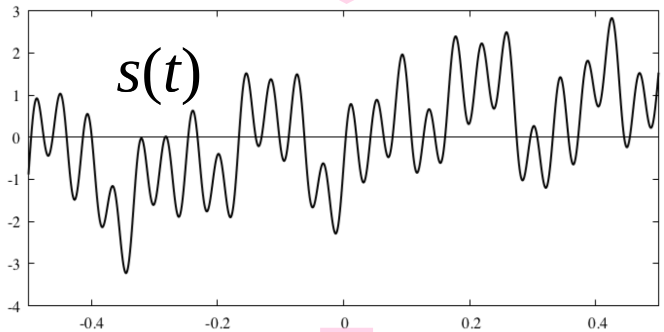

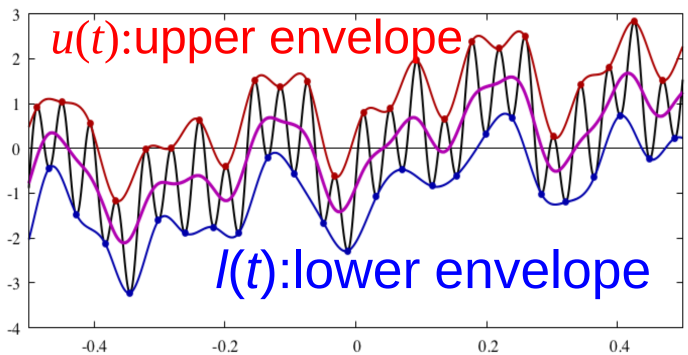

$m(t) := (u(t) + l(t))/2$

$s(t) \longrightarrow s(t) - m(t)$

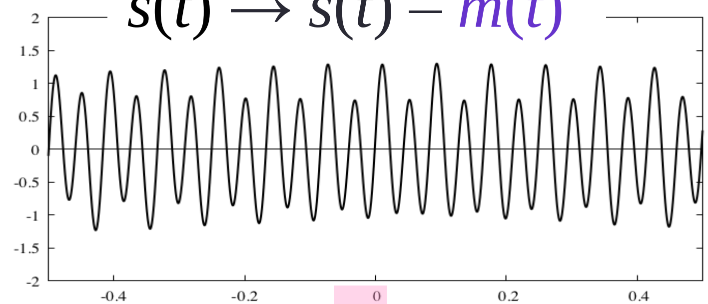

Iterate this process until $m(t)$ becomes sufficiently small

Hilbert-Spectral Analysis

$$v(t) = \frac{1}{\pi} P \int_{\infty}^{\infty} \frac{s(\tau)}{t-\tau} d\tau$$

$$a(t)e^{i\theta(t)} = s(t) + iv(t)$$

We extract f_R (from $\theta(t)$) and f_I (from $a(t)$).

The choice of initial filtering band [f_L, f_H] is a little ad hoc.

S.Yamamoto, H.Shinkai (OIT)

Fitting data in time sequence with linear function.

$$\begin{aligned} x_n &= a_1 x_{n-1} + a_2 x_{n-2} + \cdots + a_M x_{n-M} + \varepsilon \\ &= \sum_{j=1}^{M} a_j x_{n-j} + \varepsilon \end{aligned}$$

- find a_j , ε
- re-construct wave signal using the fitted function
- apply FFT to the re-constructed wave.

- The order M was fixed at 20〜30.

$P(f)$

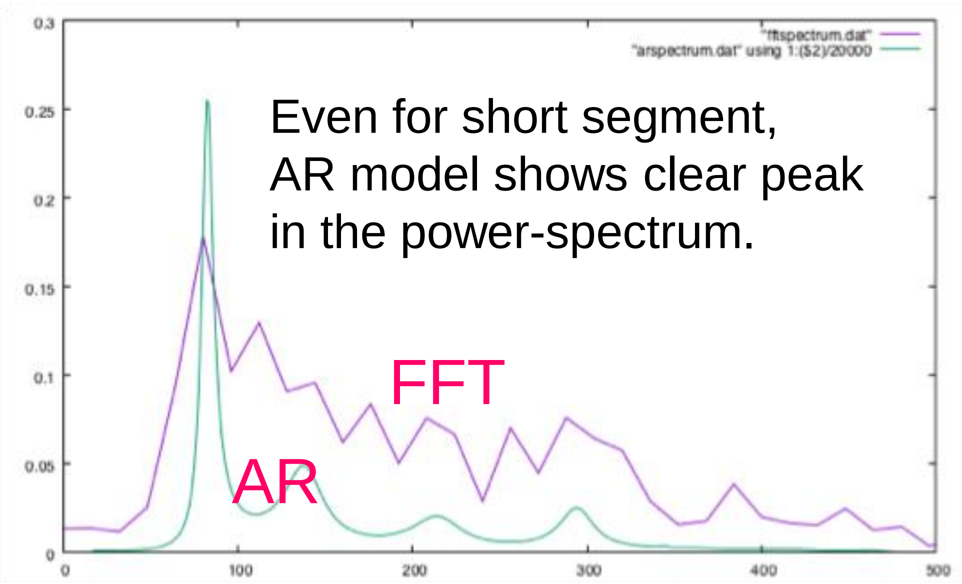

f

Convolutional neural network

Convolutional layer

$$z'_{i,l'} = \sum_{l=1}^{L} \sum_{p=1}^{H} z_{i+p,l} h^{l}_{p,l'} + b_{i,l'}$$

Pooling layer

$$z'_i = \max_{k=1,\ldots,p} z_{si+k}$$

Rectified linear unit (ReLU)

$$z' = h(z) = \max(z, 0)$$

Dense layer

$$z'_i = \sum_{j=1}^{N} w_{ij} z_j + b_i$$

layer	dimension
Input	(256, 2)
Conv	(256, 64)
Pooling	(128, 64)
ReLU	(128, 64)
Conv	(128, 128)
Pooling	(64, 128)
ReLU	(64, 128)
Conv	(64, 256)
Pooling	(32, 256)
ReLU	(32, 256)
Conv	(32, 512)
ReLU	(32, 512)
Flatten	32×512
Dense	256
ReLU	256
Dense	2
Output	2

size x channels

Choose the coefficients
h, *w* and *b*
to minimize loss function

$$J(y,t) = \frac{1}{M} \sum_{m=1}^{M} (y_m - t_m)^2$$

Challenge data

data	SNR		injected	
	$\rho_{\rm all}$	$\rho_{\rm rd}$	$f_{\rm R}^{(\rm inj)}$	$f_{\rm I}^{(\rm inj)}$
A-01	60.0	13.81	260.68	44.58
A-02	60.0	12.73	345.16	50.49
A-03	60.0	13.79	382.53	32.58
A-04	60.0	11.84	284.18	44.73
A-05	60.0	16.78	346.20	23.07
A-06	30.0	5.57	272.85	33.40
A-07	30.0	6.56	272.85	44.54
A-08	30.0	7.27	301.89	42.24
A-09	30.0	6.93	324.60	27.25
A-10	30.0	7.88	282.55	37.45
A-11	20.0	6.36	314.24	30.58
A-12	20.0	3.45	382.10	48.60
A-13	20.0	4.68	249.36	47.97
A-14	20.0	4.13	299.32	41.88
A-15	20.0	4.54	319.42	31.55
B-01	60.0	17.58	352.56	36.20
B-02	60.0	14.27	210.78	42.77
B-03	60.0	13.67	258.83	48.42
B-04	60.0	20.09	271.13	25.40
B-05	60.0	17.07	291.99	34.20
B-06	30.0	9.53	411.57	29.48
B-07	30.0	6.29	295.78	59.38
B-08	30.0	6.03	312.39	59.24
B-09	30.0	6.01	198.34	57.91
B-10	30.0	8.31	323.32	37.86
B-11	20.0	5.20	208.80	39.75
B-12	20.0	6.60	246.66	27.85
B-13	20.0	4.46	323.71	62.51
B-14	20.0	6.20	215.15	33.15
B-15	20.0	5.85	335.20	25.11

We prepared two different sets of waveform

Set-A
Set-B

- The way how we interpolate between the inspiral-merger part and the ringdown part is different.

- 15 samples for each set with various SNR for the ringdown part (3~20) are examined.

Challenge results

Error in the estimate of $\log f_R$ of $\log f_I$ (%)

		$\overline{\delta \log f_{\mathrm{R}}}(\%)$	$\sigma(f_{\mathrm{R}})(\%)$	$\overline{\delta \log f_{\mathrm{I}}}(\%)$	$\sigma(f_{\mathrm{I}})(\%)$
MF-R	A	-5.96	13.27	-49.02	78.67
	B	-14.27	18.79	-26.63	42.05
MF-MR	A	2.99	12.57	0.55	17.49
	B	2.97	5.62	5.57	15.35
HHT	A	-12.73	18.58	-49.95	63.58
	B	-9.74	16.07	-38.58	44.57
AR	A	4.93	$\boxed{10.66}$	12.85	27.44
	B	6.64	13.58	17.55	38.07
NN	A	-4.50	12.08	-13.48	29.34
	B	0.69	$\boxed{4.75}$	3.36	$\boxed{16.67}$

Set-A

Set-B

We prepared two different sets of waveform

- For matched filtering (MF-R), simple damped sinusoidal waveform was used.
- For matched filtering (MF-MR), Set-B template was used.
- Neural network (NN) was trained using Set-B template.
- Performance of MF-MR is good even for Set-A, but the error is larger for Set-A than for Set-B, as expected.
- NN exceeds the performance of MF-MR for f_R.
- For set A real part, AR showed the best performance among all.

The analysis of real data using the matched filtering-MR

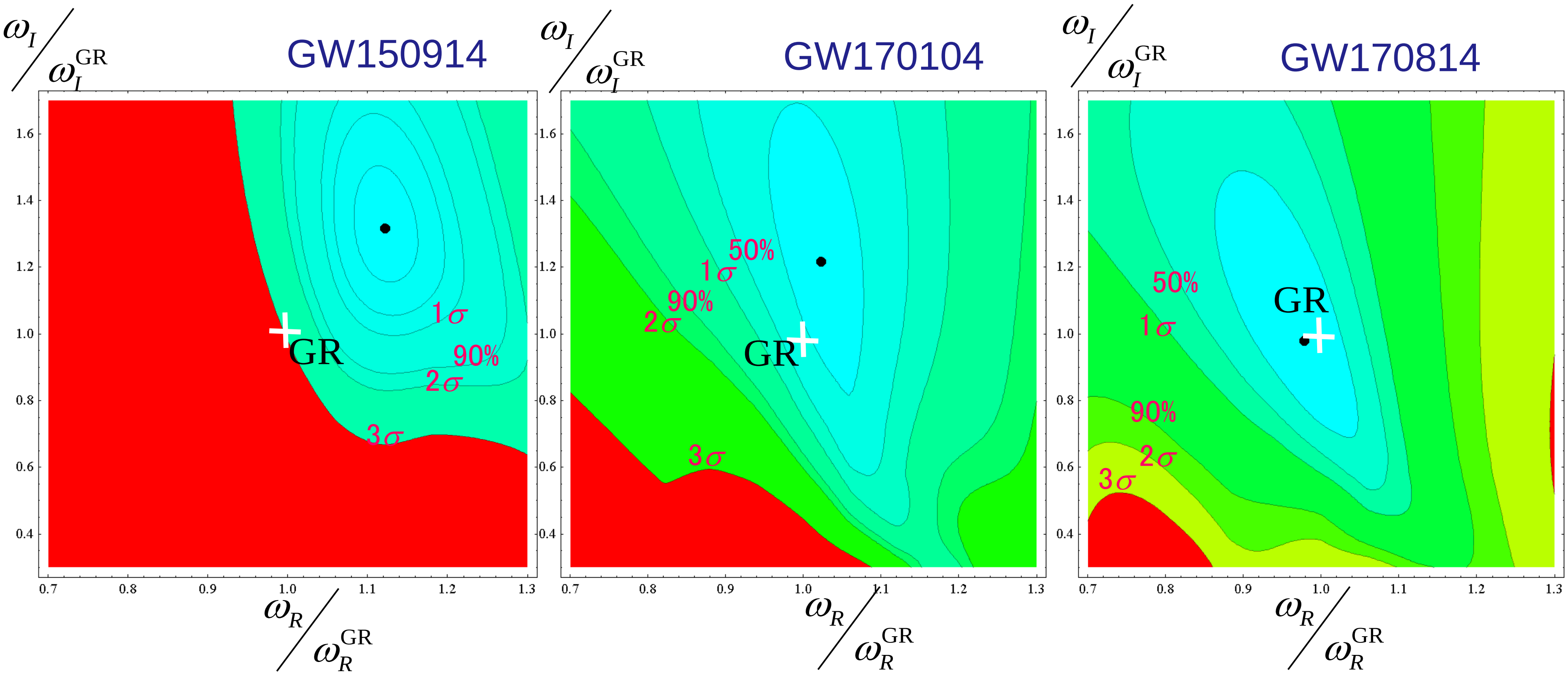

The best fit model in GR obtained from the whole data of GW150914 is on the 3σ-line obtained by the MF-MR analysis.

Ringdown wave of GW150914, GW170814, GW170104

GW150914 (S/N = 23.7)

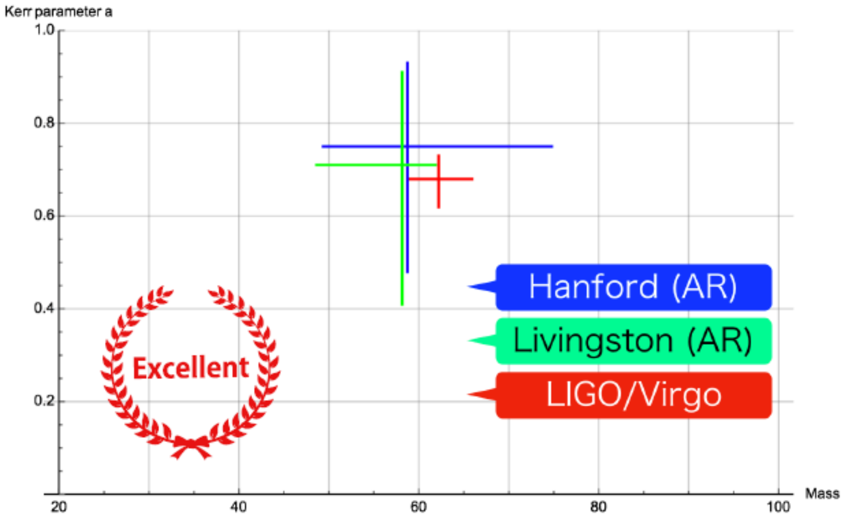

GW170814 (S/N = 18)

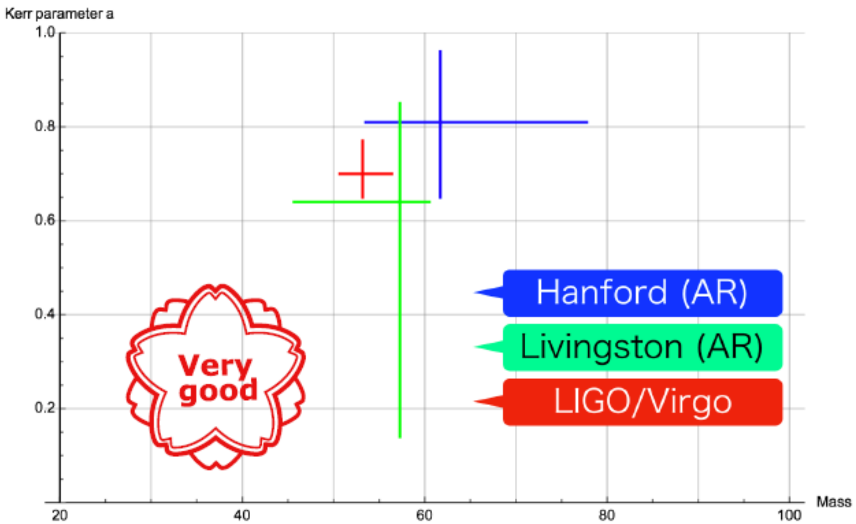

GW170104 (S/N = 13)

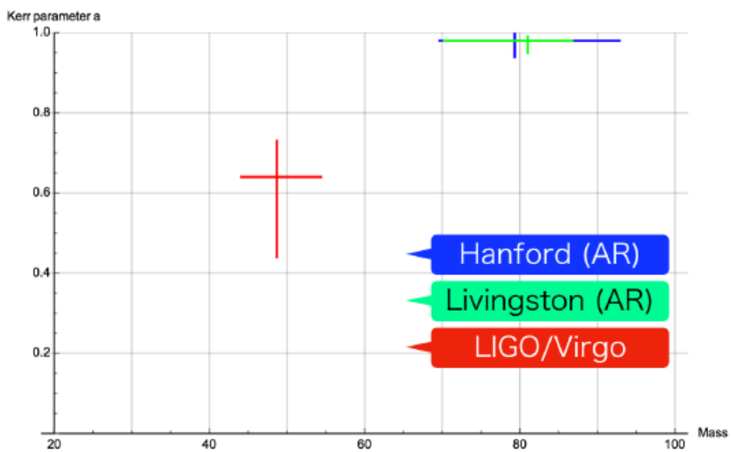

Re-analysis of Black Hole Echoes

Nami Uchikata, Takahiro Tanaka, Hiroyuki Nakano, Tatsuya Narikawa, Norichika Sago, and Hideyuki Tagoshi

BH entropy paradox

First law:

$$dM = \frac{\kappa}{8\pi G} dA + \Omega_H dJ \quad \Rightarrow \quad S_{BH} = \frac{A}{4G} \qquad \kappa = \frac{1}{2r_g} = 2\pi T$$

analogy

:Equilibrium at the Hawking temperature

Suppose matter flows continuously into BH to maintain the BH size.

The entropy emitted as the thermal radiation:

$$S_{rad} \approx T^3 A \Delta t \approx \left(\frac{M_{pl}^2}{M} \right) \Delta t$$

In the semi-classical picture, the outgoing radiation is *perfectly entangled* with the internal state of BH. $\Rightarrow$ $S_{rad} = S_{\text{insideof BH}} < S_{BH}$

After Δt exceeds the evaporation time scale $\Delta t_{evapolation} \approx t_{pl} \left(\frac{M}{M_{pl}} \right)^3$,

$$S_{rad} > S_{BH} \equiv \frac{A}{4G}$$

Possibilities

1) Hawking evaporation is wrong
2) Bekenstein-Hawking entropy bound is wrong
3) Semi-classical approximation is not valid

$\Rightarrow$ Black hole is not described by a classical spacetime

$\Rightarrow$ One may see some exotic phenomena!

There is a claim that echoes are detected from the LIGO GW events. (Abedi et al, arXiv:1612.00266)

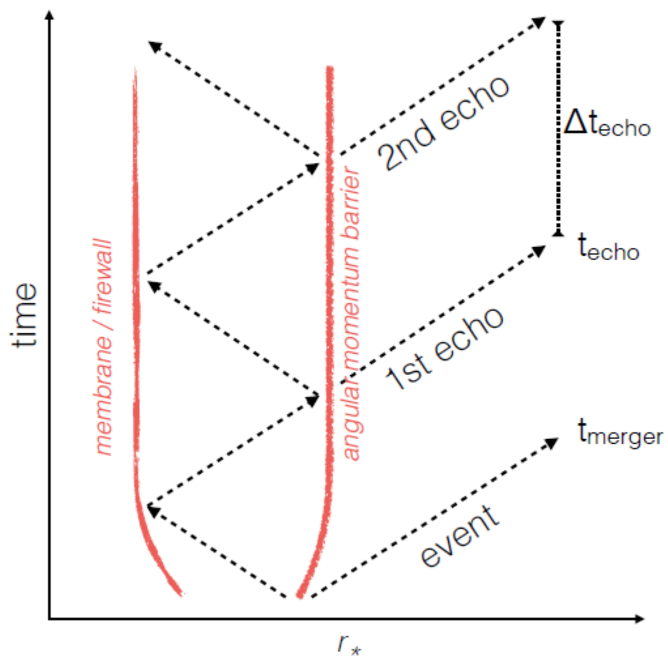

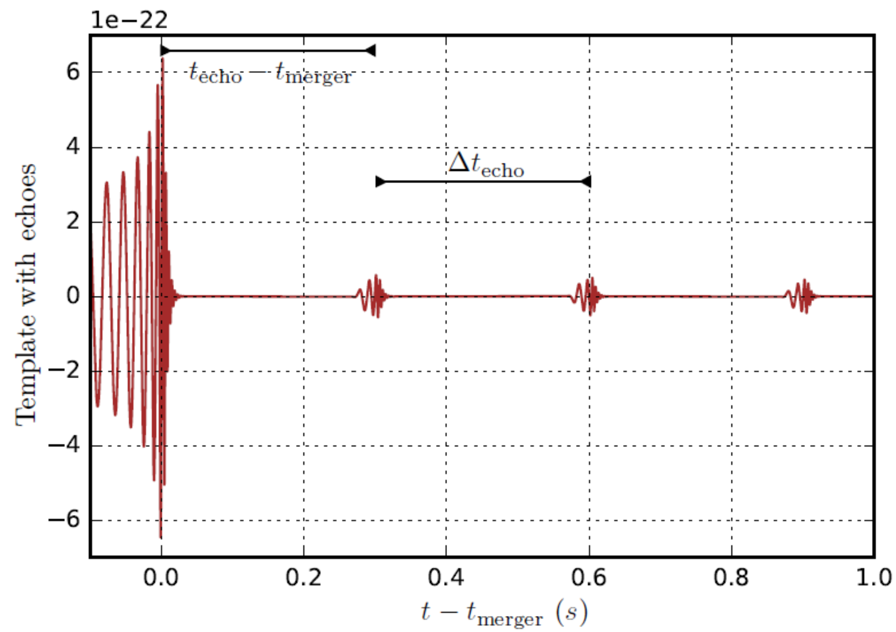

1) Reflecting boundary at the Planck distance from the horizon
2) Slowly decaying echos with predicted Δt_{echos}
3) 3σ detection of signal???

Perturbation Equation of Kerr BH (Sasaki-Nakamura) arXiv:1704.07175

We focus on the dominant mode $l=m=2$

$$\frac{d^2Y}{dr_*^2} + V_{SN} Y = 0 \quad \Rightarrow \quad Y = \begin{cases} \exp(-i\omega r_*) & (r_* \to \infty) \\ Y_{up} \exp(-ikr_*) + Y_{down} \exp(ikr_*) & (r_* \to -\infty) \end{cases}$$

Reflection rate :

$$\sqrt{\mathrm{R}(f)} = \sqrt{C}\,\frac{|Y_{up}|}{|Y_{down}|}$$

$C \neq 1$

since V_{SN} is not real

Phase shift :

$$\phi(f) = \arg\left(\frac{Y_{up}}{Y_{down}}\right)?$$

depend on the frequency f.

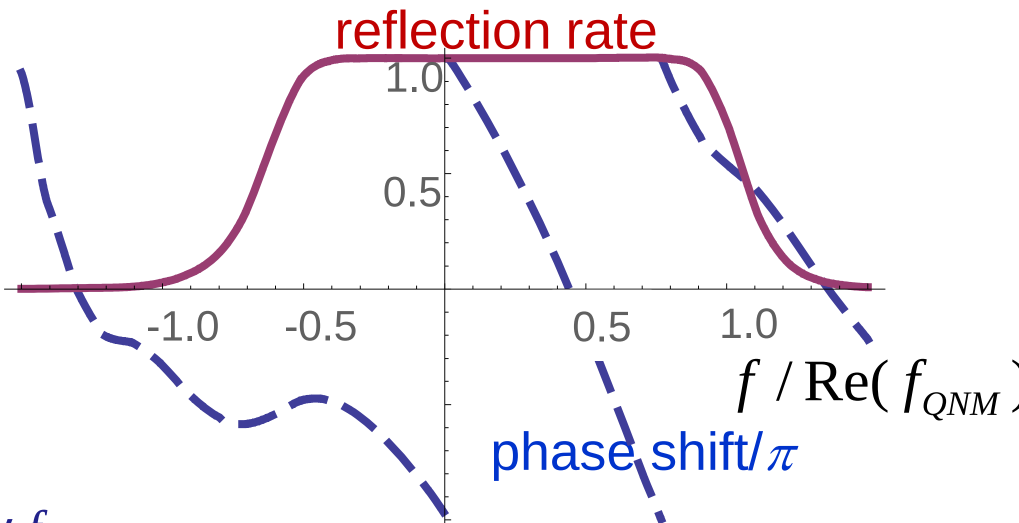

$\phi(f)$ can be approximated by a linear fn. for narrow range of f close to f_R.

$\Leftrightarrow$ $\phi(f)$ can be absorbed by time interval between echoes and the overall phase

Power spectrum changes at each reflection

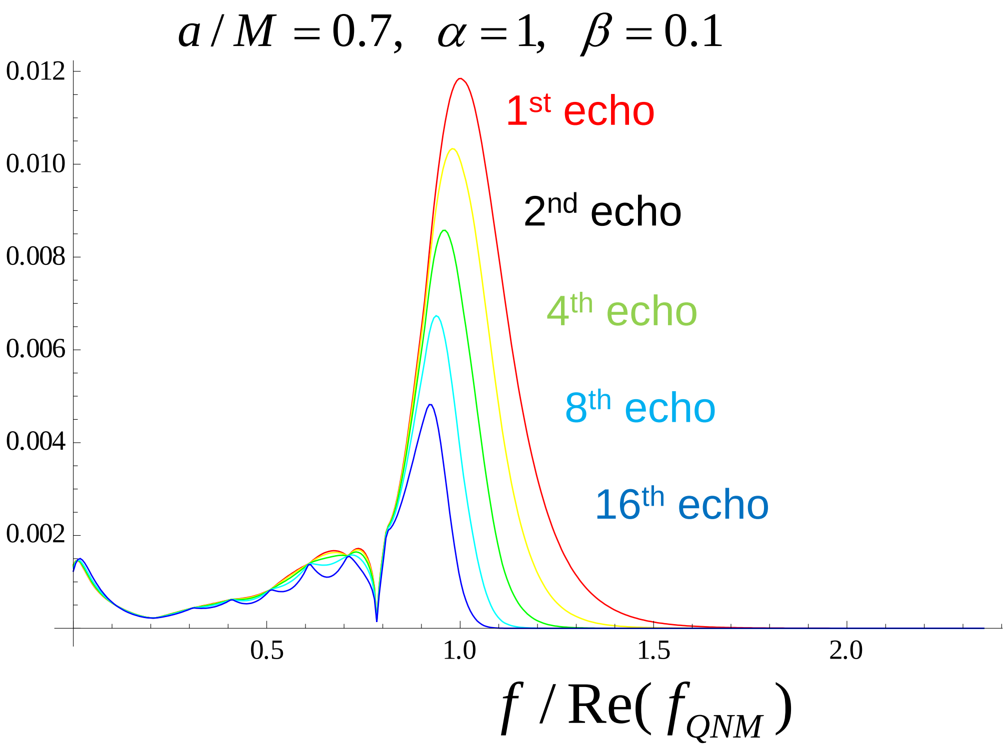

How does the significance of the echo signal change by taking into account this more physically motivated waveform?

Wave form also changes

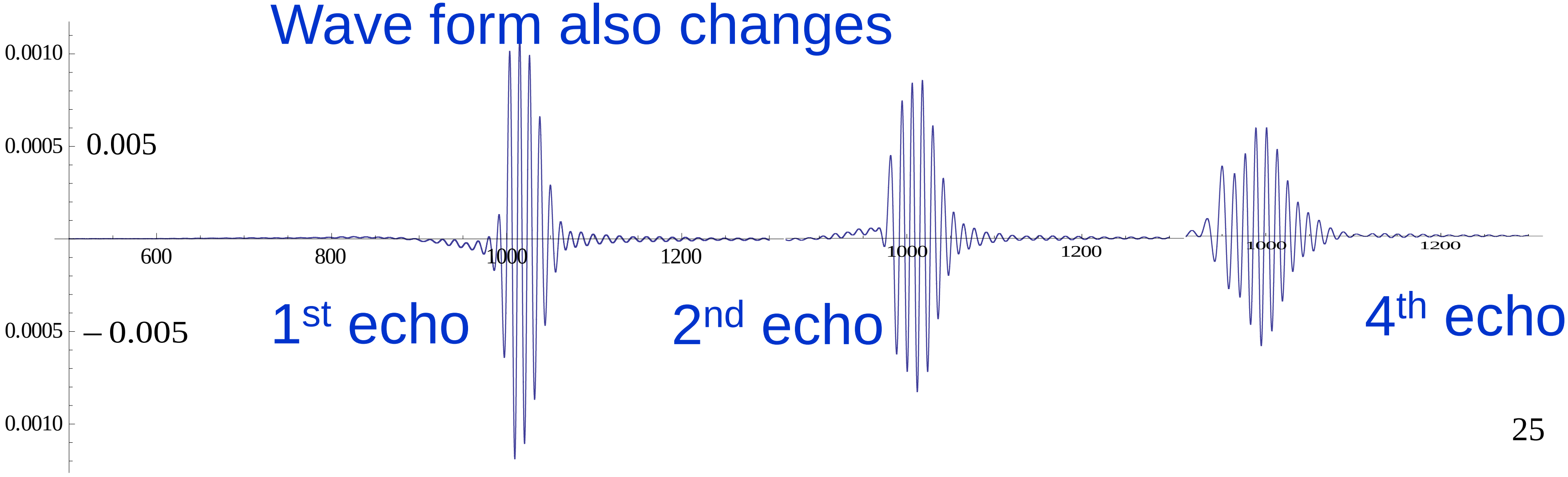

Method of analysis

We follow the basic strategy taken by Abedi et al. (2017)

Search the maximum signal-to-noise ratio (SNR) in the interval of 0.99 ≤ x ≤ 1.01, varying the other parameters.

$$x \equiv \frac{t_{echo} - \Delta t_{echo}}{\Delta t_{echo}}$$

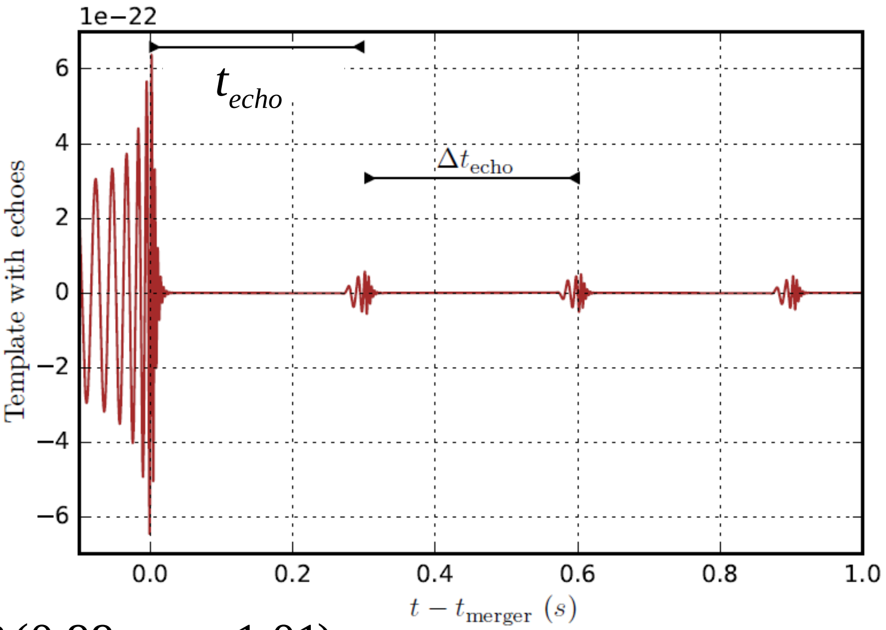

Background estimation

1) Perform the same analysis for the data at different time.

2) Perform the same analysis for the data with different *x*.

p-value

$$p \equiv \frac{\#\text{of background with SNR} > \text{SNR}(0.99 < x < 1.01)}{\#\text{of all background}}$$

If we find $p \ll 1$, there might be some true signal.

Preliminary results of our re-analysis

List of p-values

	GW150914	GW151226	GW151012	total
Westerweck et al. (2018)	0.199	0.414	0.056	0.100
Re-analysis with BG estimate 2	0.09699	0.398123	0.0203686	0.006

~2.7σ

p-value looks small but the signal is not so outstanding:

ex. LVT151012

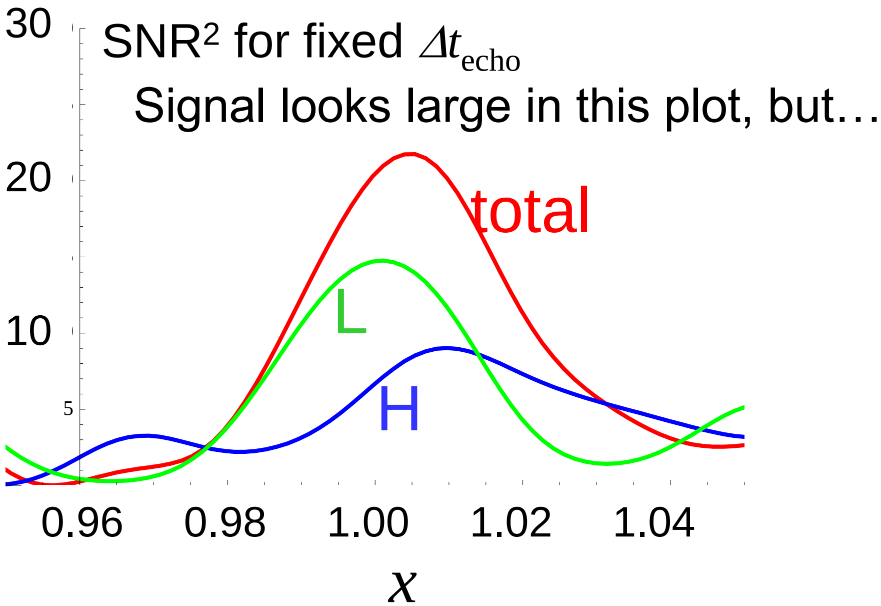

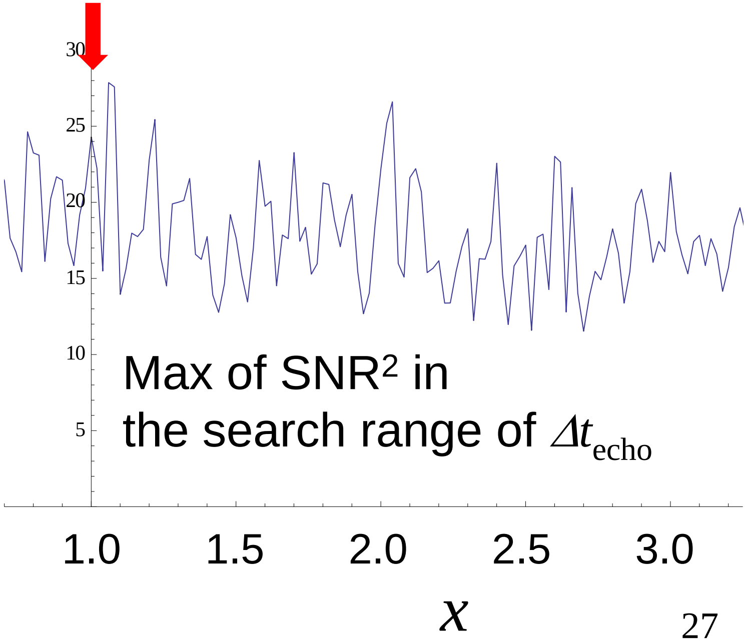

Preliminary results of our re-analysis

List of p-values

	GW150914	GW151226	GW151012	total
Westerweck et al. (2018)	0.199	0.414	0.056	0.100
background estimate 2	0.09699	0.398123	0.0203686	0.006
New template for fixed M, Q and Δφ with BG estimate 1	0.5	0.0079	0.413	
New template for fixed M and q a with BG estimate 2	0.340249	0.310848	0.0993926	0.114
New template for fixed M with BG estimate 2	0.844482	0.933738	0.101843	0.188

We could not find the expected improvement of the significance using the more physically-motivated reflection rate.

Dedicated search for signatures of specific modification of gravity

Kei Yamada, T. Narikawa, T. Tanaka …

Is PPE sufficient for the test of gravity?

$$\boxed{h(f) \approx A f^{-7/6} e^{i\Psi(f)}}$$

GW waveform from a binary in a quasi-circular orbit

$$\Rightarrow \begin{cases} A(f) \to \left(1 + \sum_i \alpha_i u^{a_i}\right) A_{GR}(f) \\ \Psi(f) \to \Psi_{GR}(f) + \sum_i \beta_i u^{b_i} \end{cases}$$

Theory	a	α	b	β
Brans-Dicke [9, 10, 14–16]	–	0	-7/3	β
Parity-Violation [22, 34–37]	1	α	0	–
Variable $G(t)$ [38]	-8/3	α	-13/3	β
Massive Graviton [8–14]	–	0	-1	β
Quadratic Curvature [23, 44]	–	0	-1/3	β
Extra Dimensions [45]	–	0	-13/3	β
Dynamical Chern-Simons [46]	+3	α	+4/3	β

(Yunes & Pretorius (2009))

There are many examples of possible extension from GR that go beyond the scope of PPE formalism.

Scalar-tensor theory without mass is strongly constrained by the pulsar timing observations.

Extra-dipole radiation gives -1PN ($(v/c)^{-2}$ relative to GR) correction.

However, the scalar field may have a small mass.

It is natural to require that the instability of the scalar field does not occur for $T_{\rm univ}$<10MeV since the effective gravitational coupling G_N must be unchanged during BBN.
This constraint suggests $m_{\rm scalar}^2 > 10^{-16}\,\mathrm{eV}$, which is comparable to the constraint from pulsar timing (PSR J0348+0432).
Grand-based detectors are sensitive to the mass range
$10^{-13}\,\mathrm{eV} > m_{\rm scalar} > 10^{-14}\,\mathrm{eV}$ (Ramazanoglu et al. 1601.07475)

If the scalar field is massive, at low frequencies there is no scalar emission and the fifth force is suppressed at a distance beyond its Compton wavelength.

There is a mass parameter region for which the dipole radiation occurs only at around the binary coalescence.

$$\phi \sim Y_{lm}(\Omega) h_l^{(1)}(kr) \int d^3x\, e^{-i\omega(t-t')} (kr)^l Y_{lm}^*(\Omega) S(x') \qquad \omega^2 = k^2 + m^2$$

$$T_{rt}^{(\phi)} \sim \phi_{,r}\phi_{,t} \sim k\omega\phi\phi$$: energy flux

For the energy loss rate due to the dipole radiation ($l = 1$),
we will have an extra factor $k^3/\omega^3 \theta(\omega - m)$ to the energy flux, compared with the well-known massless case.

Application of the test to GW150914

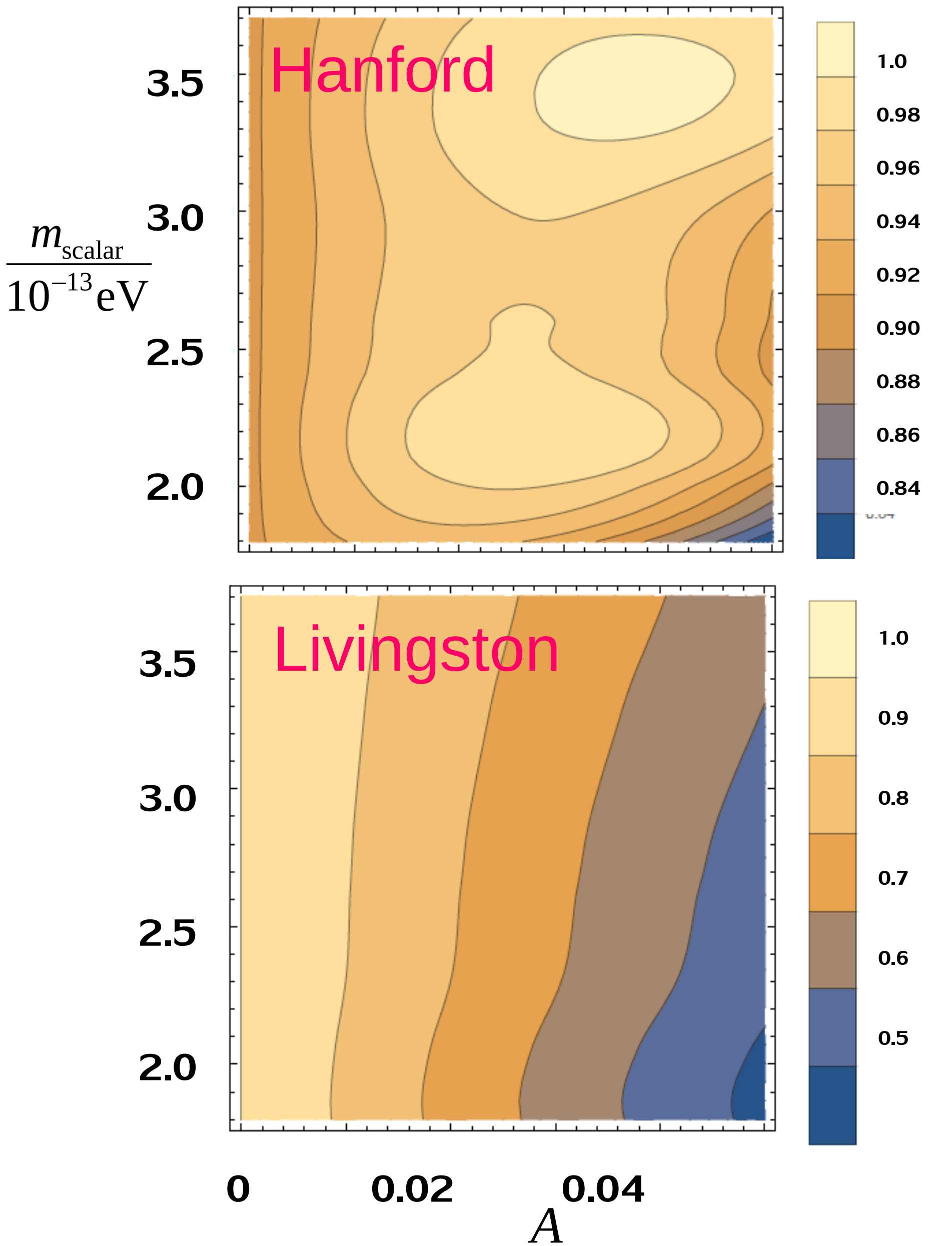

$$\left(\frac{dE}{dt}\right)_d = A\left(\frac{dE}{dt}\right)_Q \frac{k^3}{\omega^3}\Theta(\omega^2 - m^2)(2\pi f M)^{-2/3}$$

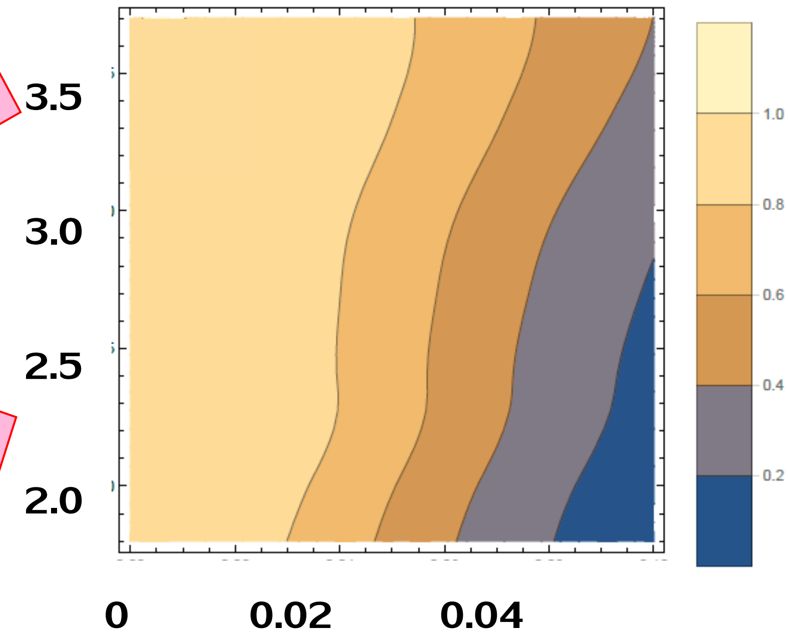

Even we introduce the scalar mass, GR is more preferred.

Summary

1) Mock data challenge for the ringdown signal has been done. Matched filtering can be biased since we do not know the waveform in modified gravity theories. Several methods can compete with the optimal matched filtering.

2) Black hole echoes have been re-analyzed by using physically more motivated waveform.
SNR increases but the signal becomes weaker.

3) We are developing rather generic library for the test of gravity using gravitational waves.
As a first step, preliminary analysis to constrain massive scalar dipole radiation has been performed.